Geothermics 131 (2025) 103358

Contents lists available at ScienceDirect

Geothermics

journal homepage: www.elsevier.com/locate/geothermics

# Top-Down Cooling and Its Role in Sustaining the Laugarnes Geothermal Field, Iceland

Adolph Bravo Jr. [a,*], Samuel Scott [a], Halldór Pálsson [b], Gunnar Gunnarsson [c,d]

[a] Faculty of Earth Sciences, University of Iceland, Iceland
[b] Faculty of Industrial Engineering, Mechanical Engineering and Computer Science, University of Iceland, Iceland
[c] Orkuveitan, Iceland
[d] Current affiliation, Baseload Power Iceland, Iceland

ARTICLE INFO

*Keywords:*
Low-temperature
Numerical model
Conceptual model
Cooling
Heat source

ABSTRACT

The Laugarnes geothermal field is a low-temperature system (<150 °C) that supplies an average of 80 $MW_{th}$ for district heating in Reykjavík. Over nearly a century of operation, the field has maintained stable pressures and discharge temperatures. Despite its longevity, the processes sustaining the reservoir's response to production are still not fully understood. This study analyzes long-term production and field data, revealing a "top-down" cooling pattern attributed to the recharge of cooler surface waters into shallow reservoir rocks. This phenomenon is then integrated into a new conceptual model of the field. Energy balance calculations – accounting for basal conductive heat flux, drawdown-induced surface recharge, and the associated cooling of the rock – demonstrate that formation cooling constitutes a significant heat source during production. A 3D numerical model, calibrated against natural-state temperature and pressure history, reproduces the observed temperature changes, further supporting the importance of heat extraction from the rock formation. The findings suggest an alternative paradigm for the understanding heat budget and transport in Laugarnes and highlight the broader relevance of recharge-driven heat extraction in low-temperature systems. Therefore, considering this process is crucial for accurately characterizing low-temperature systems and ensuring their sustainable use.

## 1. Introduction

The use of low-temperature (<150 °C) geothermal resources plays a vital role in the social and economic infrastructure of Iceland. These resources, alongside co-produced hot water derived from high-enthalpy geothermal power plants, supply hot water to district heating networks that provide about 95 % of the nation's heating needs (Axelsson et al., 2010; Ragnarsson et al., 2023). Over the past century, Iceland's strategic development of geothermal resources has significantly reduced its dependence on imported fossil fuels, contributing to energy independence and economic stability. Despite Iceland's exceptionally high per capita energy consumption – estimated at around 100 GJ per year, the highest globally – the country maintains remarkably low carbon emissions from its heating sector (Melsted, 2021; Lund and Toth, 2021). Given the critical role of geothermal district heating systems in fostering both energy security and environmental sustainability, ensuring the sustainable management of low-temperature geothermal resources remains a national priority, underscoring the need for continued research into their behavior and response to long-term exploitation.

The origin of Iceland's low-temperature geothermal systems remains debated. Unlike high-temperature fields that are linked to active magmatism, most of these low-temperature systems occur outside the volcanic belts and therefore do not have magmatic heat sources (Arnórsson, 1995). Einarsson (1966) proposed that the heat source for the low-temperature systems is solely the elevated regional conductive heat flow (ranging from 100 to 250 mW $m^{-2}$; Bodvarsson, 1982b; Flóvenz and Saemundsson, 1993), which leads to conductive temperature gradients of 50–120 °C $km^{-1}$. The water is derived from distributed recharge zones, largely located in topographically high areas, heated at depth during flow towards the lowlands, and discharged in focused upflow zones, whose locations are largely determined by favorable structural settings (Tómasson et al., 1975). Early isotopic studies suggested that water in these systems may originate from as far as 150 km away (Árnason, 1977), although later studies interpreted these signals as the result of climatic changes (Arnórsson, 1995). Implicit in Einarsson's model is the existence of a steady-state between conductive heat input and advective

* Corresponding author.
*E-mail addresses:* bravo_adolphjr@yahoo.com, ajm10@hi.is (A. Bravo).

https://doi.org/10.1016/j.geothermics.2025.103358
Received 27 February 2025; Received in revised form 15 April 2025; Accepted 23 April 2025
Available online 29 April 2025

heat output in these low temperature systems.

Simple calculations of total heat output in low-temperature fields presented by Bodvarsson (1982a, 1983) indicate that Einarsson's steady-state model cannot sustain systems with exceptionally high natural-state thermal outputs or developed fields with substantial production. For example, the Reykholtsdalur geothermal system with an the estimated natural-state advective heat output of 220 $MW_{th}$ would require that deeply circulating water is heated over an implausibly large area of 2000 $km^2$ to maintain a steady-state balance between conduction and advection. Furthermore, the observed correlation between flow rate and discharge temperature in many low-temperature systems potentially contradicts predictions of a purely conductive heat source model. Instead, Bodvarsson proposed the convective downward migration (CDM) model, where water convection within vertical fractures cools and contracts underlying rocks, facilitating fracture opening, deeper water penetration, and heat extraction at the base of the fracture. According to this model, the heat output of the low-temperature systems is controlled by the rate at which the fracture front migrates downward, alongside fracture length, fracture density, and the rock temperature at the base of the system (Axelsson, 1985; Patterson and Driesner, 2021; Halldórsdóttir et al., 2023). Heat transport in Bodvarsson's CDM model is localized in the convection cell within the fracture zone, in contrast to the expansive heat mining at depth in Einarsson's model.

Temperature measurements in low-temperature geothermal systems reveal contrasts in subsurface permeability and heat transport mechanisms (Fig. 1), often interpreted through the lens of the CDM model. Wells drilled into the upflow zones frequently exhibit near-isothermal conditions, consistent with efficient advective heat transport in high permeability rocks ($\geq 10^{-14}$ $m^2$). Conversely, some deep wells show evidence of linear temperature gradients in their deeper parts, evidence of conductive processes dominating in low permeability rocks ($\leq 10^{-16}$ $m^2$). According to the CDM model, heat extraction occurs through the downward migration of the transition between advection- and conduction-dominated zones, effectively expanding the vertical extent of the near-isothermal zone. As a result of the extensive near-isothermal zone that often extends down to 2 km depth, temperatures in the upper ~1 km of these systems are elevated relative to the regional conductive gradient, while temperatures in the deeper parts of these systems fall below it.

The phenomenon of heat extraction by fluid flow and transient permeability creation in initially low permeability hot rock has been referred to as "thermal mining" (Tómasson and Arason, 2000). By assuming that subsurface temperatures in low-temperature geothermal systems initially followed a normal conductive gradient, the net heat extracted from rocks is calculated based on the difference between the heat content of rock under a normal conductive gradient (Fig. 1, well 3) and the actual heat content derived from wellbore temperature measurements (Fig. 1, well 1). While this approach aligns with the framework of the CDM model, it oversimplifies the inherently three-dimensional nature of these geothermal systems. Vertical temperature profiles, such as those from wellbores, primarily reflect the distribution of permeability and large-scale fluid flow dynamics, rather than the system's overall heat transport efficiency. For example, a vertically extensive isothermal zone indicates high permeability over a wide depth interval, but this local thermal signature and its deviation from the regional conductive gradient do not directly correlate with the efficiency of heat transport for the entire system. Fully understanding heat transfer dynamics requires accounting for the three-dimensional pathways of fluid recharge and upflow and their relationship to the permeability structure and potential heat sources at the system scale.

Both the purely conductive heat flow model and the CDM model overlook a related potential source of thermal energy: the heat extracted from rock along distributed recharge pathways. This process shares some conceptual similarities with the "stored heat" method of resource capacity estimation. This method assumes that geothermal systems contain inherent thermal energy within the reservoir that gets extracted during production (Grant and Bixley, 2011). Various versions of the method are compared by Quinao and Zarrouk (2014). Essentially, the heat extraction is governed by the volume of the reservoir, the temperature change, and the porosity-permeability structure of the rock. The magnitude of heat extracted could represent a significant heat source for the systems that are fed by these recharge zones. For example, cooling 1 $km^3$ of rock by 1 °C over one year generates a thermal energy flow rate of ~70 $MW_{th}$. While the mechanism of energy extraction from stored heat along distributed recharge pathways clearly shares some similarities with the CDM model and the related "thermal mining" concept, it differs in that heat extraction from rock is not confined to the base of a convection cell within a fracture. Instead, heat can be extracted wherever cooler recharging water interacts with hotter rock, broadening the range of potential heat sources in low-temperature geothermal systems. This heat source will potentially become more significant during production, as reservoir depressurization triggers recharge of colder waters into the hotter reservoir rock.

In this study, we examine thermal energy stored in the rocks as another potential heat source, by incorporating it in the energy balance and heat transport process in the Laugarnes field. Our focus on Laugarnes stems from the comparatively rich and long-term production history of the field, indicating stable discharge temperatures despite production averaging ~150 L $s^{-1}$ over the past five decades. Close examination of temperature measurements from wells reveal significant cooling in the shallower sections of the system, which we interpret as indicative of local recharge and heat extraction from the shallow

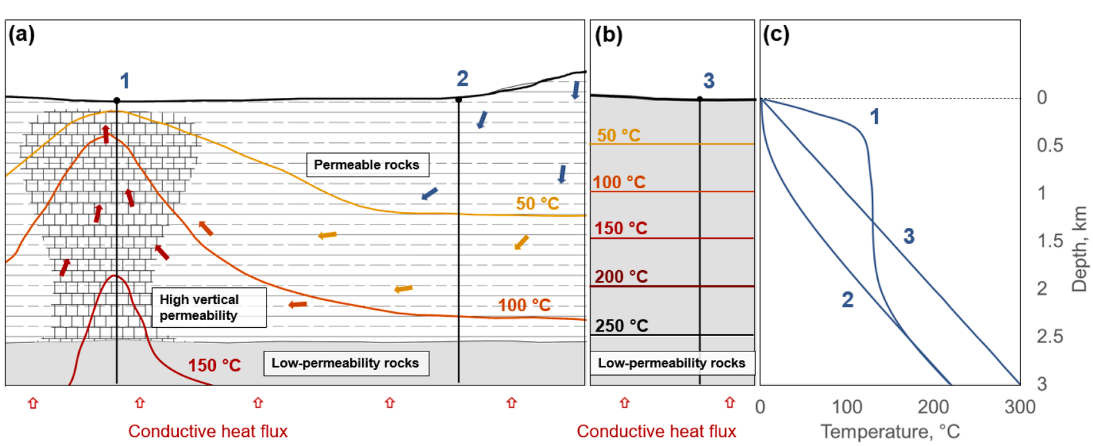


**Fig. 1.** (a) Heat transport in geothermal systems based on conductive heat flux and that is largely controlled by permeability distribution, (b) expected conductive gradient in low-permeability rocks, and (c) temperature profiles of wells drilled in (1) upflow zones, (2) recharge zones, and (3) low-permeability rock formations.

portions of reservoir. To test this model quantitatively, we developed a 3D numerical model of the field calibrated using the long-term production data. The model reproduces the natural state thermal structure of the system solely from the elevated regional conductive heat flux as well as the phenomenon of heat extraction from rock at shallow depths in response to production. We thus describe an alternative to the CDM model in explaining both the origins of low-temperature geothermal systems in Iceland as well as the processes that govern the thermal response of reservoirs to production.

## 2. The laugarnes geothermal field

Laugarnes is one of three low-temperature geothermal fields in the Reykjavík area developed for hot water production, alongside Seltjarnarnes and Elliðaár (Fig. 2). The Reykjavík area, situated approximately 10 km north of the active Reykjanes rift zone, is underlain by Tertiary and Quaternary rock formations, mainly subaerially erupted basaltic lava flows, subglacially erupted hyaloclastites, and basaltic intrusions (Tómasson et al., 1975). The geothermal systems are situated on the southern margin of the extinct Viðeyjar caldera, with Laugarnes located at the intersection of the caldera rim and a NW-SE fissure zone (Gunnlaugsson et al., 2000; Arnórsson, 1995; Arnórsson et al., 1992). Impermeable barriers, likely consisting of NW-SE-oriented dykes and associated faults, are thought to separate the three hydrothermal systems and limit hydraulic connectivity between them (Thorsteinsson and Elíasson, 1970; Tómasson et al., 1975; Tómasson, 1993).

The stratigraphic sequence at Laugarnes, based on drill cuttings from wells analyzed by Thorsteinsson and Elíasson (1970) and later by (Friðleifsson, 1990), reveals alternating layers of basalt flows, pyroclastics, and sediments extending to depths of up to 2.2 km. The largest feed zones are primarily located at the contacts between lithologic layers (Tómasson et al., 1975). Alteration mineralogy studies of wells drilled in Laugarnes, as well as in the nearby Elliðaár field, indicate high-temperature alteration, implying former temperatures exceeding 230 °C (Friðleifsson, 1982; Yaowanoiyothin, 1984; Tómasson, 1993; Kristmannsdóttir, 1975).

The development of Laugarnes for hot water production in 1930 marked the start of large-scale geothermal energy utilization in Iceland. Initial developments of the field included drilling of shallow wells near the thermal springs to increase hot water production, followed by the construction of a 3-km pipeline to distribute the hot water to the eastern parts of Reykjavík. This infrastructure laid the groundwork for the city's district heating system, which soon expanded to include a larger network of residential and commercial buildings (Gunnlaugsson et al., 2000). Presently, Reykjavík, along with surrounding municipalities, relies extensively on this system, with half of the hot water demand met by five low-temperature fields and the remainder by two high-temperature co-generation plants within the Hengill system (Thorbergsson et al., 2023).

The production history of Laugarnes from 1930 to 2022 is shown in Fig. 3. Prior to its large-scale utilization, the hot springs discharged 5–10 L $s^{-1}$ of water at approximately 87 °C. In 1930, 14 shallow wells (<250 m) were drilled near the Þvottlaugar hot spring, increasing the discharge to 15–20 L $s^{-1}$. Over the following years, additional shallow wells were drilled, increasing the total capacity of the field. During this period, production relied entirely on artesian flow from the wells. A significant increase in hot water production occurred in 1960 with the introduction of rotary drilling. The larger diameter wells allowed for the installation of downhole pumps, boosting production and accessing deeper, more productive sections of the reservoir. Production continued to rise with increasing demand in the succeeding years, peaking in 1990. However, it was subsequently reduced following the initiation of hot water production from Nesjavellir, one of the two high-enthalpy co-generation power plants, and to mitigate the effects of observed groundwater influx,

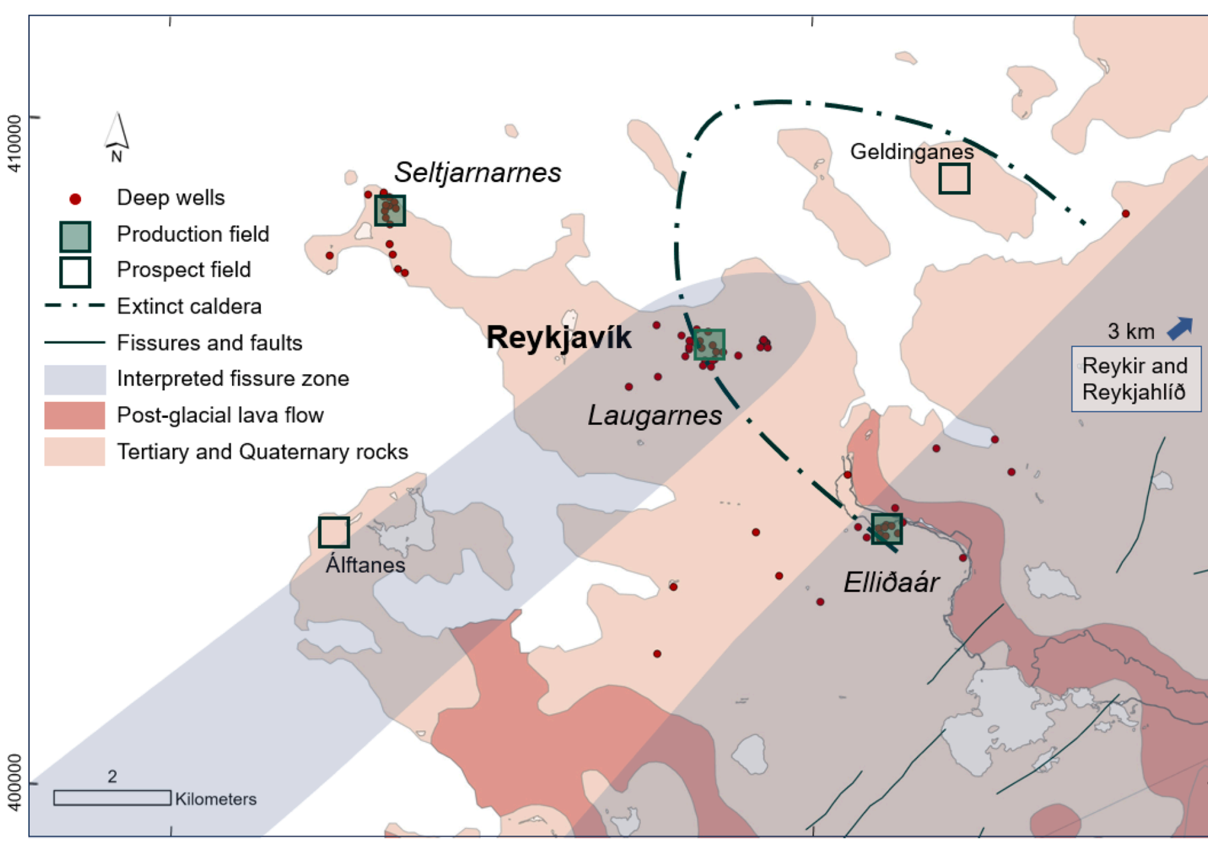


**Fig. 2.** Low-temperature geothermal systems in the Reykjavík area.

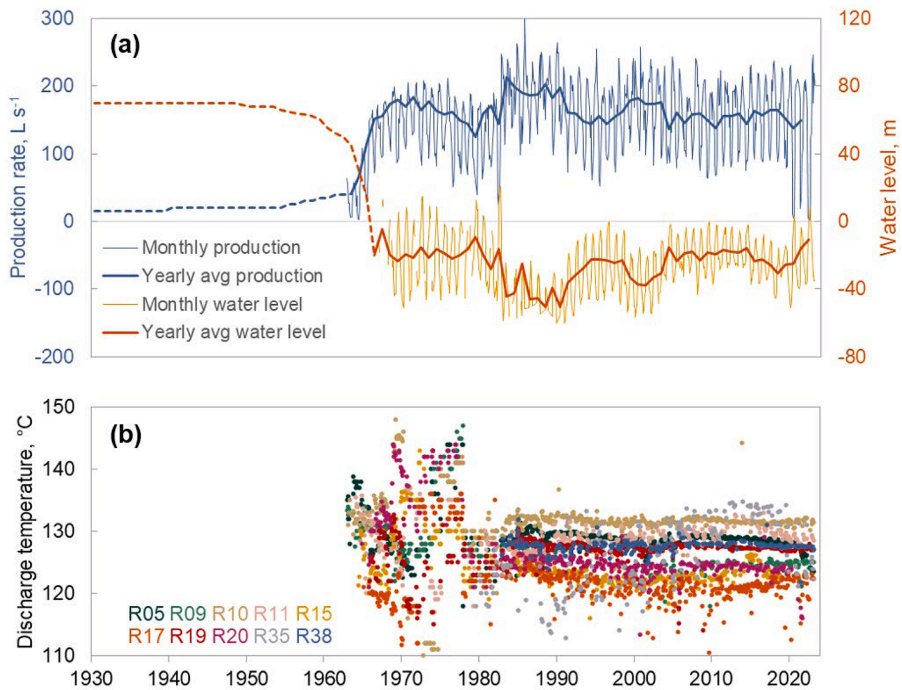


**Fig. 3.** Production history of the Laugarnes low-temperature system. (a) Production rates and water levels, and (b) Discharge temperature measurements from the Laugarnes wells. Note that the data before 1980 is unreliable.

evidenced by increasing Cl concentrations and decreasing Si concentrations. For the next three decades, production in Laugarnes was maintained at an annual average of 160 L $s^{-1}$, with notable seasonal fluctuations (Gunnlaugsson et al., 2000; Axelsson et al., 2010). This production is equivalent to about 80 $MW_{th}$ assuming recharge of 5 °C.

Water levels in the Laugarnes field exhibit a clear correlation with production levels over both short and long timescales. Monthly average water levels (Fig. 3a) exhibit seasonal fluctuations primarily driven by hot water demand, which peaks in winter and allows for recovery during off-peak periods. Yearly averaged water levels similarly correlate with long-term production trends. Initially, reservoir pressure was estimated at 6–7 bar at sea level, supporting self-flowing wells and hot springs. However, the introduction of downhole pumps in the 1960s significantly increased production, leading to a rapid water level decline of approximately 120 m Despite this sharp drop, long-term water levels have since stabilized as production rates became more consistent. Seasonal fluctuations remain the dominant variation, with the reservoir reaching a quasi-equilibrium where natural recharge balances extraction (Axelsson, 2010).

Interpreted formation temperatures obtained from Laugarnes wells show a distinct pattern (Fig. 4): a high conductive gradient from the surface to a depth of 500 m, followed by an isothermal zone maintaining temperatures around 130 °C down to approximately 2200 m This isothermal zone indicates high permeability, consistent with inferred permeabilities of $\sim 10^{-14}$ $m^2$ from analytical models (Bodvarsson and Zais, 1981; Björnsson et al., 1990; Changhong, 2012) and the observation that approximately 80 % of the production is derived from aquifers at depths of 730 to 1250 m below sea level (Thorsteinsson and Elíasson, 1970). In the deepest well, R34, a conductive gradient reappears below the isothermal zone at 2200 m depth, extending to the bottom of the well. This suggests lower permeability in this section, marking the base of the permeable resource. As previously noted, the downward migration of this zone could support the hypothesis of moving fracture front and heat extraction from progressively greater depths, consistent with the CDM model. However, repeat temperature surveys from R-34 are not available to confirm this interpretation.

Björnsson et al. (1999, 2000) proposed a conceptual model of

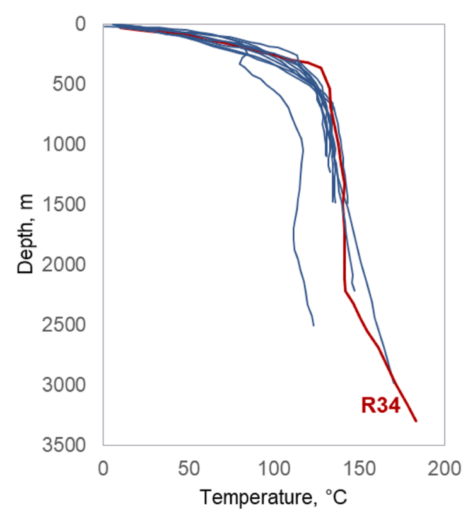


**Fig. 4.** Interpreted formation temperatures of the Laugarnes wells based on static temperature surveys (Björnsson et al., 1999).

Laugarnes by mapping interpreted formation temperatures in Laugarnes (Fig. 4) and in other geothermal systems surrounding Reykjavík (Fig. 2). The resulting temperature distribution showed localized temperature maxima in all the geothermal systems and indicated possible locations of cold and hot recharge influencing their temperature distributions. According to this model, Laugarnes is fed by hot water originating from as far as 20 km northeast. This hot water flows at depth until it encounters vertical permeability beneath Laugarnes, where it ascends (Fig. 5). This interpretation aligns with the fracture-controlled water convection described in the CDM model.

Quantitative models of Laugarnes (Thorsteinsson and Elíasson, 1970; Bodvarsson and Zais, 1981; Axelsson, 1989; Fendek, 1992; Sarak et al., 2005; Changhong, 2012) have predominantly focused on forecasting the field's pressure (water level) response to production. In many of these models, an open or unconfined boundary condition is assumed to resolve

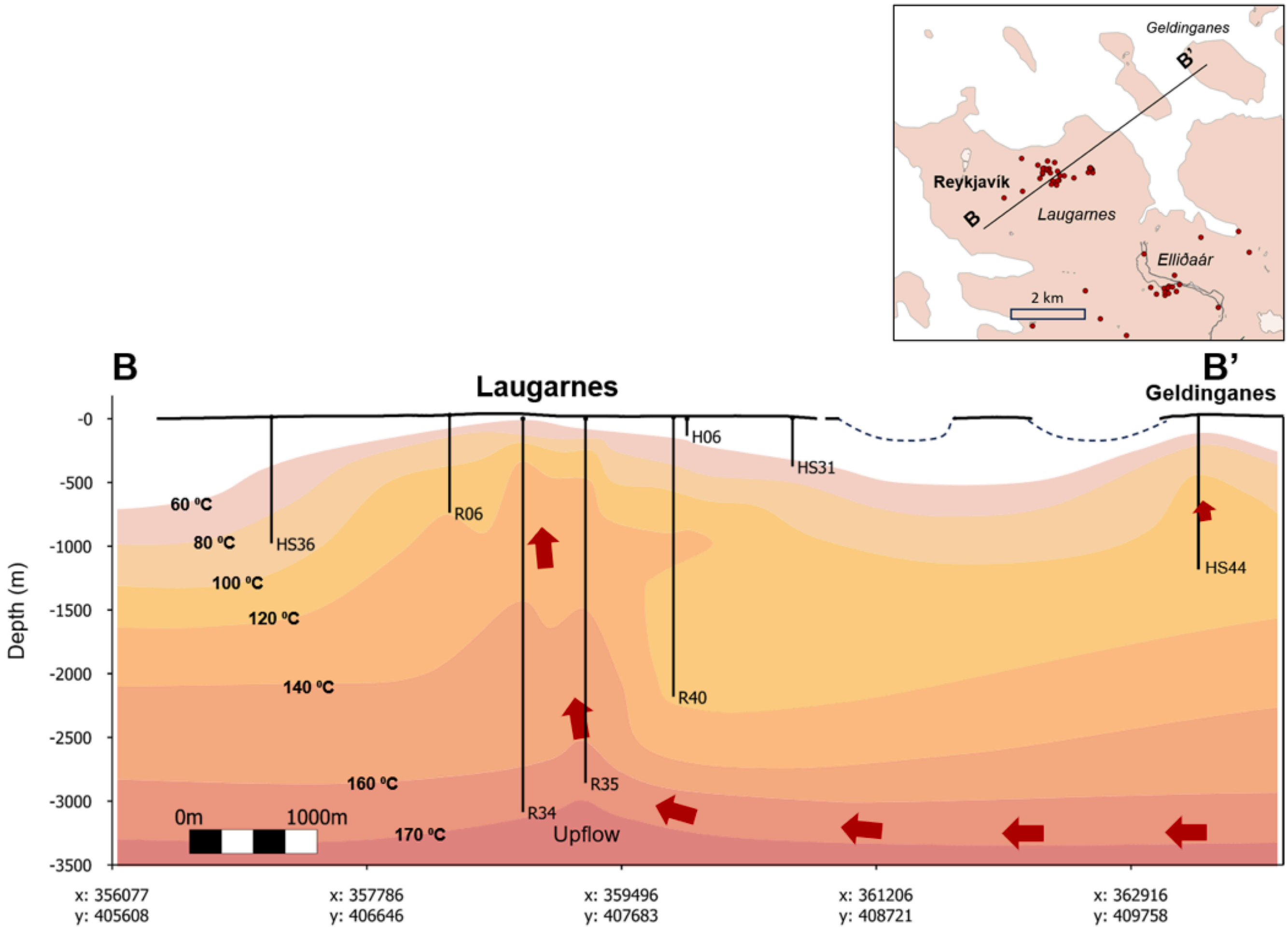


**Fig. 5.** SW-NE cross-section of the conceptual model of Laugarnes, showing the interpreted hot water recharge from the NE. Redrawn from Björnsson et al. (1999, 2000).

the stability in water level. As shown in Fig. 3b, long-term measurements indicate that the discharge temperatures have also remained remarkably stable over several decades. This observed stability has led earlier studies to emphasize pressure response to water extraction, often excluding considerations of thermal energy balance. As a result, these models project stable discharge temperatures alongside reservoir pressure, without accounting for potential long-term thermal depletion.

The overall mass and energy balance of the conceptual model described in Fig. 5 is challenging to reconcile if the hot water in the system relies exclusively on deep recharge. In such case, the stability observed in the water levels and discharge temperatures implies that the deep recharge must be at constant pressure and temperature. However, such a boundary condition also implies an infinite source of hot water. Consequently, this model predicts that the field will sustain indefinitely under future scenario simulations (O'Sullivan and O'Sullivan, 2016). This assumption also suggests an unlimited energy supply for Laugarnes, meaning that increased extraction would simply result in the field providing more water. As a result, forecasting the sustainability of Laugarnes becomes challenging, as the field's limits cannot be clearly defined.

## 3. Methods

### 3.1. Well data

Orkustofnun, the National Energy Authority (NEA) of Iceland, maintains a comprehensive database of all wells drilled across the country, including detailed records on drilling history, coordinates, depth, and various surveys conducted on these wells (https://www.map.is/os/). The publicly accessible database provided relevant well data and static temperature surveys for wells located in and around the Reykjavík area. Björnsson et al. (1999) also compiled the well data, including temperature surveys available up to 1999.

To evaluate formation temperatures in the Laugarnes field and possible changes over time, we analyzed well completion dates, survey dates, and temperature profiles, selecting only surveys suitable for accurate interpretation. Surveys conducted before or shortly after well completion were excluded because the wells were likely still stabilizing. Additionally, surveys indicating dynamic processes – such as flowing conditions, those with interzonal flow, or erratic data – were excluded to avoid misrepresenting formation temperatures. Only stable static temperature surveys were used to interpret the formation temperatures of the field.

For wells with more than one stable static temperature survey, the earliest valid survey was designated as the baseline, with subsequent surveys categorized as follow-ups to evaluate temperature changes at various depths. Of the more than fifty wells drilled in and around Laugarnes, only thirteen had usable temperature surveys for assessing temperature changes. The remaining wells were excluded from the analysis due to the presence of only heat-up surveys or erratic follow-up data, which limited the ability to accurately calculate temperature changes over time.

Orkuveitan, the operator responsible for the production and distribution of hot water in Laugarnes through its subsidiary Veitur provided historical production data of the field. The dataset includes monthly averages of pumping rates, discharge temperatures, and static water levels collected from 1960 to present. Production data prior to 1960 were sourced from Axelsson (2010).

### 3.2. Numerical model

We developed a numerical model of the Laugarnes geothermal system using the Volsung software package (version 2.2.20240815) created by Flow State Solutions. The numerical method is similar to that of TOUGH2 (Franz and Clearwater, 2021), and the governing equations are detailed in Clearwater and Franz (2019). The “water+air” equation of state (EOS), also referred to as EOS3 in other geothermal simulators (O’Sullivan et al., 2013), was used to account for the influence of the atmospheric block that is the model’s upper boundary.

A simplified geological model of the field was created using Leapfrog™ Geothermal 4.0. The inputs included a downloadable digital elevation map of Iceland from the National Land Survey of Iceland (Landmælingar Íslands, https://www.lmi.is/), well coordinates, elevation and drilled depth data from Orkustofnun, and simplified lithostratigraphic cross-sections of Laugarnes and Elliðaár from Thorsteinsson and Elíasson (1970) and Tómasson (1993). Lithologic units were categorized into three layers – upper basalts (<500 m), hyaloclastites (500–1000), and lower basalts (>1000 m) – based on these studies. To align with the flat-layered structure of the numerical grid, the base of the hyaloclastites was assumed to be flat, rather than slightly dipping to the southeast as described in the original lithostratigraphy.

Using Leapfrog and PyTOUGH (Croucher, 2011), we generated a 20 km by 20 km simulation grid centered on Laugarnes. The grid was oriented at an azimuth of 45° to align with potential flow paths identified in the conceptual models (Björnsson et al., 2000; Tómasson, 1993). The numerical grid consists of 15,352 blocks (Fig. 6a). Horizontal grid resolution ranges from 1 km on the outer margins of the model to 0.5 km at the center. Vertical layer thicknesses are 100 m in the topmost 1 km (layers 2–11), 250 m in the next kilometer (layers 12–15), and 500 m in the two deepest layers (layer 16–17). The grid also encompasses the low-temperature geothermal fields in Elliðaár, Seltjarnarnes, and even the nearby prospects in Álftanes and Geldinganes.

To simplify permeability calibration, new rock types were defined to represent the reservoirs at Laugarnes and Elliðaár, each with three lithologic layers. The same layer thicknesses were applied to the global lithologic structure. The two hydrological barriers separating Seltjarnarnes, Laugarnes, and Elliðaár were implemented as distinct lithologic units. To illustrate all the units, a NW-SE (DD’) cross-section through the middle of the grid is presented in Fig. 6b The properties of each unit are summarized in Table 1.

The model applied boundary conditions at the bottom and top of the model domain. At the base of the model (layer 17), a conductive heat flux of 0.15 to 0.20 W $m^{-2}$ was specified, consistent with the regional conductive heat flow (Flóvenz and Saemundsson, 1993). Blocks at the top of the model, representing the ground surface, are connected to an atmospheric block at a fixed pressure and temperature, as suggested by O’Sullivan and O’Sullivan (2016). The blocks corresponding to the ocean were also assigned a fixed temperature and constant hydrostatic pressure, with depths estimated from bathymetry data.

Manual calibration of the numerical model was carried out through

**Table 1**
Properties and calibrated permeability values of the lithologic units in the numerical model.

| Unit | Density (kg $m^{-3}$) | Porosity | k(x) | k(y) | k(z) |
|---|---|---|---|---|---|
| Laugarnes UB | 2700 | 0.075 | 1.45e-14 | 1.8e-14 | 8.5e-15 |
| Laugarnes H | 2700 | 0.075 | 1.45e-14 | 1.8e-14 | 8.5e-15 |
| Laugarnes LB | 2700 | 0.075 | 1.35e-14 | 1.5e-14 | 7.0e-15 |
| Upper Basalts | 2700 | 0.075 | 1.2e-14 | 1.3e-14 | 3.0e-15 |
| Hyaloclastites | 2700 | 0.075 | 1.2e-14 | 1.3e-14 | 3.0e-15 |
| Lower Basalts | 2700 | 0.075 | 1.1e-14 | 1.2e-14 | 2.7e-15 |
| Laugarnes Barrier | 2700 | 0.075 | 1.0e-16 | 1.0e-15 | 1.0e-16 |
| Elliðaár Barrier | 2700 | 0.075 | 1.10e-15 | 1.0e-15 | 5.0e-16 |
| Elliðaár UB | 2700 | 0.075 | 1.30e-14 | 1.1e-14 | 6.0e-15 |
| Elliðaár H | 2700 | 0.075 | 1.30e-14 | 1.1e-14 | 6.5e-15 |
| Elliðaár LB | 2700 | 0.075 | 1.20e-14 | 1.0e-14 | 6.5e-15 |

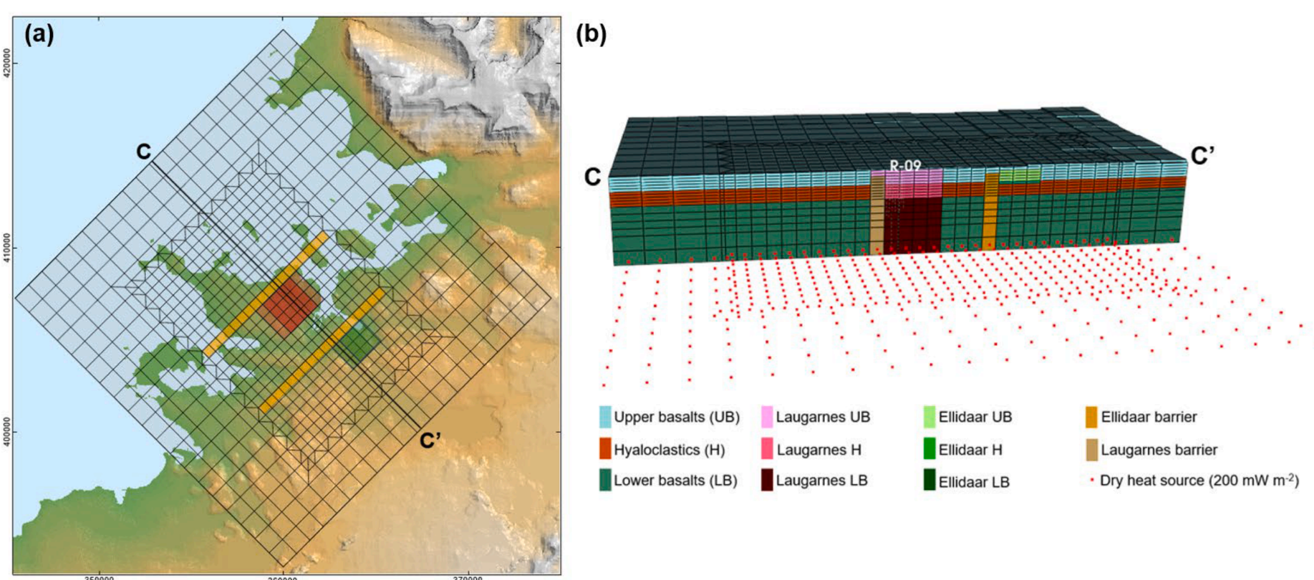


**Fig. 6.** Numerical model of the Laugarnes low-temperature geothermal reservoir, showing (a) extent of the numerical grid overlaid on topographic relief, and (b) a cross-section of the grid, showing the layer thicknesses and the new lithologic units implemented for reservoir blocks in Laugarnes.

an iterative two-step process following O'Sullivan and O'Sullivan (2016), adjusting the anisotropic permeabilities ($k_x$, $k_y$, $k_z$) of the lithologic units. First, natural-state calibration was performing by matching the resulting block temperatures with the static formation temperatures obtained from well surveys. A natural state was considered achieved when the mass and energy balance equations were satisfactorily resolved for a time step of at least 1 million years, indicating steady-state conditions. Next, a production history calibration was performed, and the rock permeabilities were further adjusted accordingly to achieve a reasonable match with the historical water levels from monitoring wells. Note that water level measurements were obtained from well R05 until 1985, after which time they were recorded from well R07. This process was repeated iteratively until the modeled natural-state temperatures and historical reservoir pressures closely aligned with measured data with a single set of rock permeability values.

Note that although the numerical model was calibrated using water level data, it does not directly simulate water table levels – a limitation arising from the selected top boundary condition. Some numerical studies (e.g., Ratouis et al., 2016; Beaude et al., 2019) have successfully implemented boundary conditions that allow for water table simulation. However, these approaches require either an extremely fine top grid mesh or specific formulations that are not feasible with the software used in this study. Consequently, they were not implemented. This may potentially influence the permeability calibration. Nevertheless, if the pressure drawdown primarily occurs in the blocks where mass is extracted and is then distributed to surrounding blocks, it is possible to estimate the pressure drop of a well intersecting these blocks using the following equations. First, the pressure for each block n under column a is converted to their equivalent hydrostatic head according to:

$$H_{a,n} = \frac{P_n}{\rho g} - z_n \tag{1}$$

$P_n$ is the pressure of block $n$ under column $a$, $\rho$ is fluid density, $g$ is gravitational acceleration, and $z_n$ is the block center depth from sea level. In calculating water level in the manner, we assumed a constant water density of approximately 940 kg/m$^3$ (corresponding to a temperature of 120 °C). The water level of column a $(H_a)$ is then taken as the average of the hydrostatic pressures of underlying blocks:

$$H_a = \frac{\sum H_{a,n}\Delta t_n}{\sum \Delta t_n} \tag{2}$$

where $\Delta t_n$ is the block thickness. Essentially, the water level in column a is calculated by averaging the hydrostatic pressure of the blocks underneath but taking into account the thickness of the blocks. Furthermore, only blocks 4 ($z_n = 250\ m$) through 13 ($z_n = 1325\ m$) were considered as these blocks account for the majority of the feed zones in the reservoir (~95 %).

Once calibrated, the numerical model was used to test the discharge temperature of a modeled well and compare it with actual discharge temperatures. The productivity indices (PIs) of the feed zones in the modeled wells were assigned values listed in Table 2. These values align with the field-wide production distribution estimated by Thorsteinsson and Elíasson (1970), with 15 % of the feed zones located in the shallow section (300–600 mbsl), 80 % in the intermediate section (600–1400 mbsl), and only 5 % in the deep section (>2000 mbsl).

## 4. Results

### 4.1. Formation temperature changes

Repeat measurements of formation temperatures in Laugarnes indicate transient cooling at shallow depths (<1 km), but near-constant temperatures at greater depths. Fig. 7 illustrates the calculated changes in formation temperature ($\Delta T_r$) from the 13 wells in Laugarnes that have more than one stable static survey. For wells that have reached

**Table 2**
Assumed feed zones and permeability indices of a modeled well based on field-wide feedzone distribution from Thorsteinsson and Eliasson (1970).

| Feed zone depth, m | PI (Fixed) |
|---|---|
| 350 | 0.05 |
| 450 | 0.05 |
| 550 | 0.05 |
| 650 | 0.10 |
| 750 | 0.10 |
| 850 | 0.10 |
| 950 | 0.10 |
| 1050 | 0.10 |
| 1150 | 0.10 |
| 1250 | 0.10 |
| 1350 | 0.10 |
| 2000 | 0.05 |

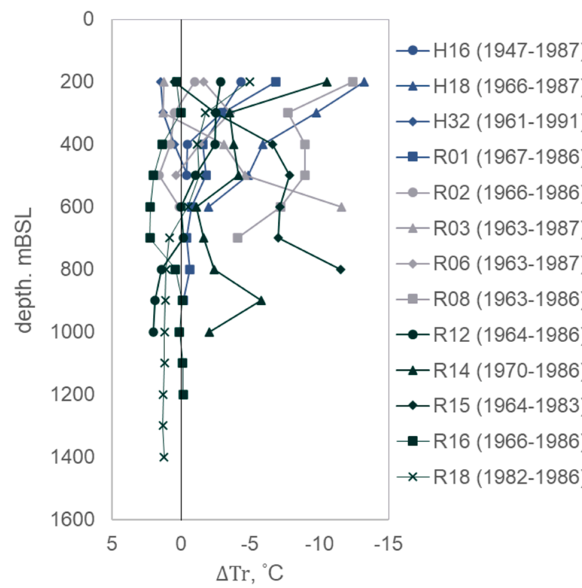


**Fig. 7.** Calculated formation temperature changes in Laugarnes wells based on static temperature surveys.

depths of 1000 m (such as R14, R15, R16, and R18), deep formation temperatures remain stable, with variations within 2 °C. In contrast, significant cooling up to 15 °C is observed in the shallower sections of many wells. At a depth of 500 m, temperatures have decreased by up to 10 °C. Fig. 7 further illustrates that this cooling effect diminishes with increasing depth, highlighting the stability of formation temperatures in the deeper sections compared to the shallower zones.

### 4.2. Thermo-hydraulic structure of laugarnes

The calibrated numerical model effectively reproduces the natural-state temperature distribution in Laugarnes, the evolution of water in Laugarnes in response to production, and the near-constant discharge temperatures of the production wells. The calibrated anisotropic permeabilities of the various lithologic units are shown in Table 1, which generally range between $10^{-16}$ and $10^{-14}$ m$^2$. The calibration indicates lower vertical permeability than horizontal permeability both for the global and reservoir rocks. Note that although Elliðaár lies within the model boundaries, it was excluded from the calibration. The field is close to the edge of the high-resolution section of the grid, and expanding this section would have required increasing the model size and consequently, the computing power needed. Calibrating including Elliðaár would have also required more time to match the natural-state temperatures and production history pressures of the field alongside that of Laugarnes. Similarly, Seltjarnarnes and the two low-temperature prospects (Fig. 2) were excluded for the same reason.

Fig. 8 illustrates the natural-state temperature distribution from the numerical model, highlighting an upflow feature under Laugarnes. This is further illustrated in Fig. 9 where the modeled temperature surveys of wells near the center of the reservoir closely match the interpreted formation temperatures from static surveys. Convective temperature profiles appear in both the modeled and measured temperatures, particularly within the productive depths of the reservoir (500–2200 m), where the model reproduces the temperature of the isothermal zone of 130–140 °C. However, slight discrepancies in temperatures were observed in the shallow sections (<300 m), where the model temperatures were higher by as much as 20 °C, and in the deeper sections (>2500 m), where the modeled temperatures were lower by 10–20 °C. Wells drilled further from the center, such as R38 and R40 (Fig. 9e-f), also showed lower modeled temperatures compared to the measured formation temperatures. A closer match of the temperature profiles could potentially be achieved by fine tuning the permeabilities of the lithologic units, for example by introducing new units along the fringes of the reservoir to better match R38 and R40. Nevertheless, the numerical model satisfactorily reproduces the upflow at the correct temperature in the productive section of the field.

The thermal structure in Fig. 8 indicates that the primary natural-state flow of water follows the topographic gradient from the southeast, converging at Laugarnes, where it encounters higher vertical permeability. This upward flow is further enhanced by an adjacent low-permeability barrier, which directs more flow upward rather than laterally through it. Shallow cold recharge from the southeast is also apparent, indicated by temperature patterns that align with the inferred recharge direction. In contrast, there is little to no deep flow from the northeast (Fig. 8, BB'), although the model indicates a northeastward and a slight southwestward outflow in the shallower sections.

Fig. 10 compares the historical water level measurements from monitoring wells with calculated water levels from the calibrated numerical model. At the start of production, the modeled reservoir pressure, averaged across all reservoir blocks and adjusted to ground level using a hot hydrostatic gradient, was ~1 bar higher than the actual recorded values, corresponding to a water level of 80 m. Despite this initial discrepancy, the model effectively replicated the rate and magnitude of the decline observed in 1960 following the rapid increase in production. The modeled reservoir pressure also sufficiently replicated the stabilization of the water level in the succeeding years, as well as the accurately capturing subsequent fluctuations in water levels following variability in production (Fig. 3).

The numerical model reproduces the pattern of cooling in Fig. 7, with stable temperatures at the depth of production zones and cooling at shallow depths. Fig. 11a shows the evolution of block temperatures in Column A, where about half of the production wells are located, from 1900 to 2020. Initially, temperature decline is not evident, particularly during 1900 to 1930, when only natural discharge existed, and 1930 to 1960, when production levels were relatively low. However, from 1960 to 1990 and then to 2020, significant cooling becomes evident, especially in the shallower blocks, while the deeper blocks remain thermally stable. This is shown clearly in Fig. 11b, which compares the modeled temperature decline the decline measured from the wells shown in Fig. 7. In calculating these changes, we consider the period from 1960 to 1990, during which most of the temperature surveys in Fig. 7 were conducted. Additionally, the surrounding columns B, C, and D show similar temperature decline that is higher in depths above 500 mbsl.

Simulated formation temperature changes suggest relatively rapid cooling at shallow depth but slower decrease at greater depth and slower decrease in production temperatures. Fig. 12 shows the evolution of block temperatures of Layers 7 and 12 in the central part of the reservoir, representing the shallow and deeper sections of the system, respectively. To predict the future performance of the field, we used the model to forecast block temperature that if production is maintained for another

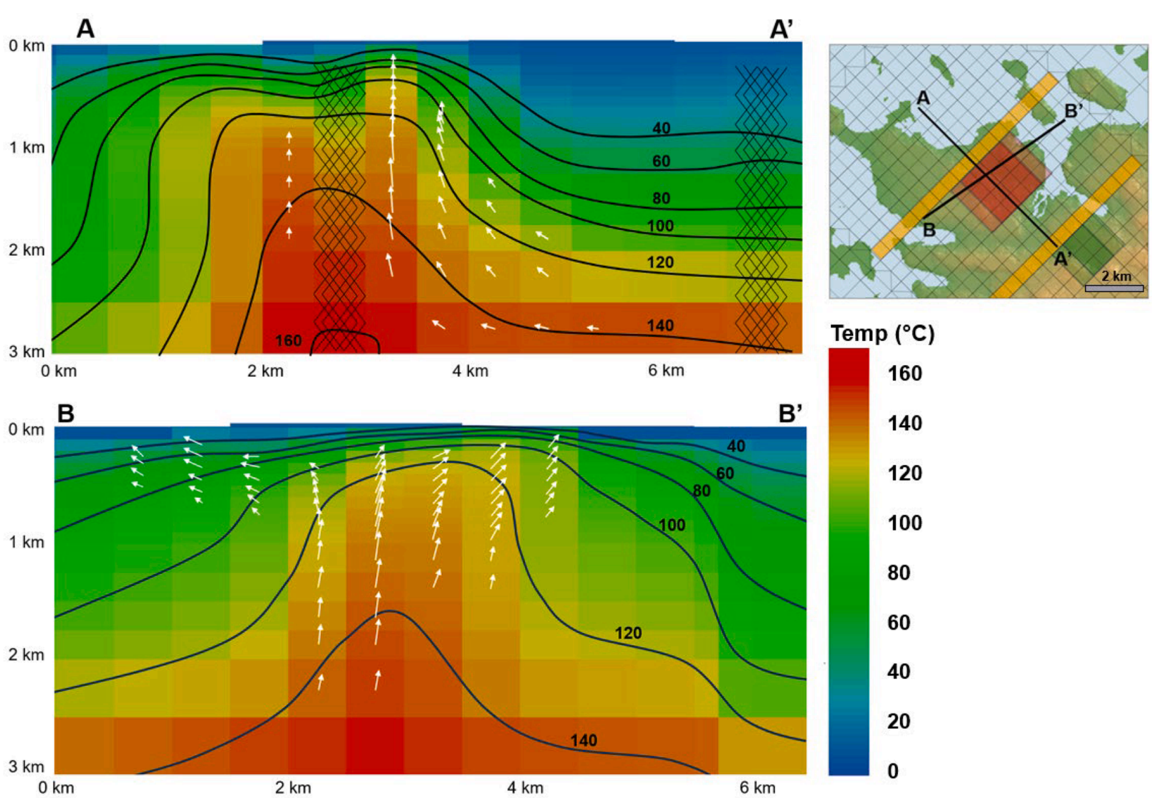


**Fig. 8.** (AA') NW-SE and (BB') SW-NE cross-sections showing the natural-state temperature distribution from the numerical model – the blocks are colored according to calibrated temperatures, while the white arrows represent the magnitude and direction of water flow velocity from the blocks.

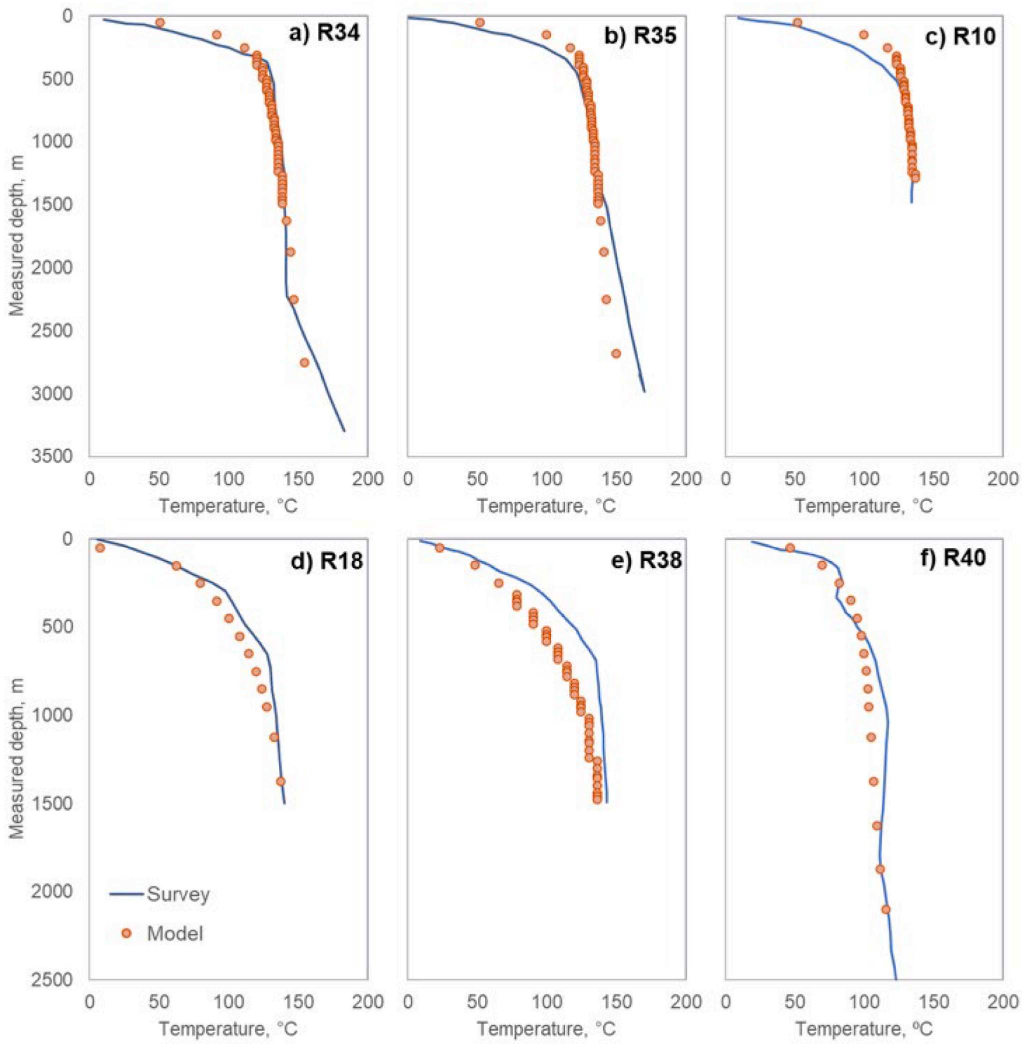


**Fig. 9.** Comparison of modeled natural-state temperatures and interpreted formation temperatures from static temperature surveys.

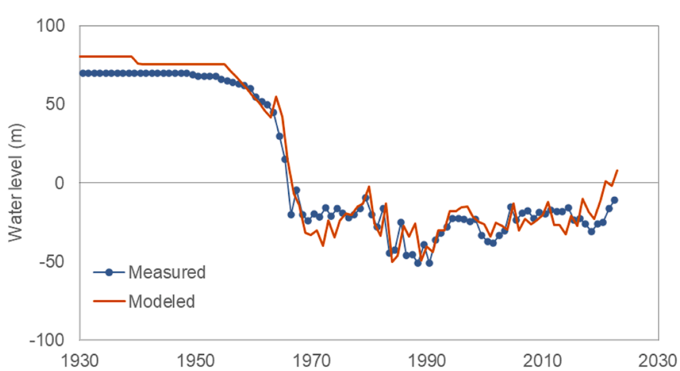


**Fig. 10.** Comparison of water levels measured from R05 and R07, and the simulated water level from the model.

100 years (Scenario 1). The model predicts that Layer 7 will significantly cool down by as much as 25 °C, while Layer 12 will experience a more modest decrease of only about 2 °C. In Scenario 2, where production is stopped, temperature regeneration occurs in both shallow and deep layers, though it is slow. After an additional 100 years without production, block temperatures remain below the pre-production levels.

Despite the decrease in the modeled block temperatures, the discharge temperature of the modeled production well shows a relatively slow decline. In Fig. 12b, the modeled well's discharge temperature decreased by only 5 °C, with an expected further decline of 7 °C over the next 100 years of continued production. This decline is similar in magnitude to what is observed in some production wells, such as R05 and R19. This highlights that while the discharge temperatures of production wells have remained nearly constant, there is still a noticeable decline in some of the wells when considering the broader context.

## 5. Discussion

### *5.1. "Top-Down" cooling and shallow recharge at laugarnes*

Repeat temperature measurements from the Laugarnes field suggest that the system is experiencing production-induced cooling from the "top-down", i.e., beginning at shallow depths and progressing to greater depths with time (Fig. 7). Although production temperatures remain constant (Fig. 3), temperature changes shown in Fig. 7 highlight that the effect of production on reservoir temperatures is evident by a decline in static formation temperatures in the upper 500 m of the system. While most baseline surveys were conducted in the 1960s, when production levels were low as pumping had just begun, follow-up surveys performed 20 to 30 years later, during a period of significantly higher production, suggest that the observed temperature changes can be attributed to the sustained high extraction levels. In Fig. 8, temperatures in the deeper sections of the reservoir (below 1000 m) remain stable, indicating

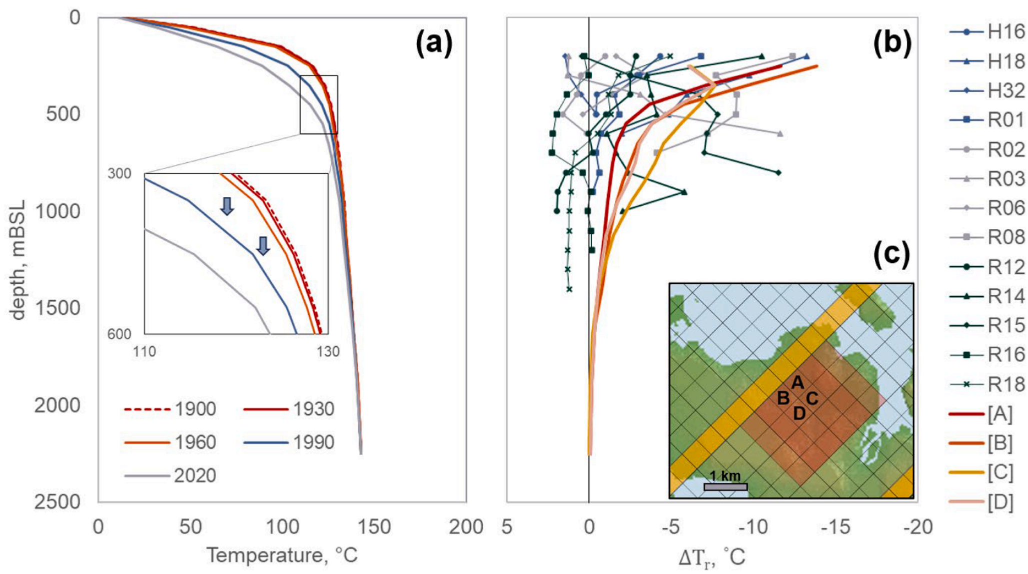


**Fig. 11.** (a) Evolution of block temperatures in Column A over time, highlighting a decline in shallow temperatures following production, (b) comparison of modeled temperature changes in the central reservoir columns with temperature changes observed from wells, and (c) location of the columns evaluated.

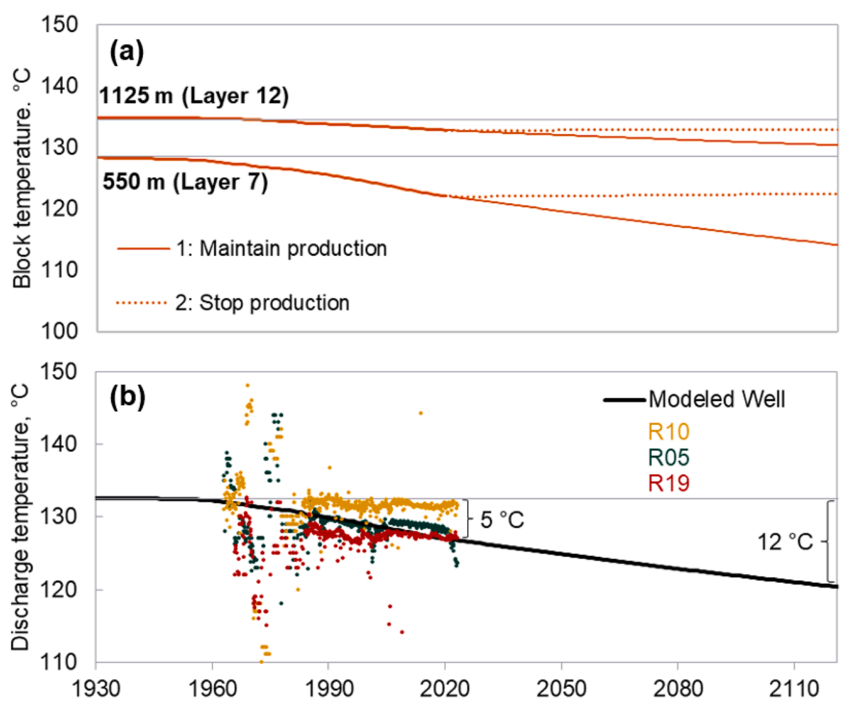


**Fig. 12.** a. Predicted block temperatures for shallow (layer 7) and deep (layer 12) blocks Scenario 1 (maintain production) and Scenario 2 (stop production), and b. Predicted discharge temperature of a modeled production well under Scenario 1 (maintain production) compared to measured discharge temperatures from two production wells.

minimal impact from production.

The cooling pattern in Fig. 7 suggests an influx of cold recharge from near-surface areas, which extracts heat from near-surface rocks as it flows downward towards the production zones. As this colder recharge absorbs heat from the rock, increasing water temperature while decreasing the temperature of the rock, it gradually approaches a state of thermal equilibrium with the rock in the deeper sections of the reservoir, reducing its capacity for further heat exchange. Thus, cooling is restricted to shallow depths while deeper temperatures are constant. Note, however, that not all wells show this cooling trend, e.g., wells R02, R03, R15, and R16. These variations in cooling could help pinpoint the primary direction or sources of cold recharge. However, the limited number of surveys and the differing intervals between them – ranging from 4 years (R18) to 30 years (H16, R01) – make it difficult to accurately track the spatial and temporal variability in temperature decrease. Moreover, the last temperature surveys were obtained >3 decades ago, and more recent measurements of stable formation temperatures should show larger cooling. Nonetheless, these findings suggest that cooling is induced by local cold recharge (downflow of surface waters), which should be incorporated into the mass and energy balances of the system and considered in both conceptual and quantitative models.

Simple calculations based on the decline of formation temperatures suggests that the heat extracted from the rocks is sufficient to maintain the overall energy balance in the field during production. We evaluate this by establishing a thermal balance of the system during production (Eq. (3)), where the total heat produced by the reservoir is expressed as the sum of heat input from various source: basal conduction ($Q_{conduction}$), stored heat in the formation ($Q_{in\text{-}place,\ rock}$), heat of the in-situ water ($Q_{in\text{-}place,\ water}$), and heat from deep aquifer recharge ($Q_{upflow}$), according to the proposed mechanism:

$$Q_{produced} = Q_{conduction} + Q_{in-place,\ water} + Q_{in-place,\ rock} + Q_{recharge} \tag{3}$$

Assuming a system that is closed to deep recharge, this equation can be written as:

$$mtC_w(T_{prod} - T_{ref}) = qtA_{Res} + V_{reservoir}\phi\rho_w C_w(T_{res,init} - T_{ref}) + V_{reservoir}(1-\phi)\phi\rho_r C_r(T_{res,init} - T_{res,prod}) \tag{4}$$

The left-hand term of Eq. (4) represents the heat produced from the field over its entire productive life. This is calculated based on the mass flow rate ($m$), productive life ($t$), density of water ($\rho_w$), the heat capacity of water ($C_w$), and the temperature difference ($\Delta T_w$) between the average discharge temperature ($T_{prod}$) and a reference temperature ($T_{ref}$), assumed to be the ambient temperature of 5 °C. $Q_{conduction}$ is calculated from the conductive heat flux (q) flux of 200 mW m$^{-2}$ heating the reservoir area ($A_{Res}$). The heat content of the in-situ water can be calculated based on, reservoir volume ($V_{reservoir}$), porosity ($\phi$), the density of the water ($\rho_w$), the heat capacity of water $C_w$, and the difference between the reservoir temperature ($T_{res,init}$) and the reference temperature. Similarly, the heat taken from the formation is calculated based on reservoir volume, porosity, the density of the rocks $\rho_r$, the heat capacity of the rock $C_r$, and the temperature change in the formation occurring due to production ($\Delta T_r$). To simplify, we assume that the mass taken out from the system is fully replaced by recharge, according to the pressure response of the field during production. This recharge must sufficiently equilibrate with the rocks to sustain near-constant discharge temperatures, and therefore, must be heated to $T_{res,prod}$. Consequently, the energy to heat the recharge is drawn from the other two sources. The last two terms in Eq. (4) can then be combined:

$$mtC_w(\Delta Tw) = qtA_{Res} + hA_{Res}(\phi\rho_w C_w + (1-\phi)\phi\rho_r C_r)\Delta T_r \tag{5}$$

In Eq. (5), only two heat sources remain: basal conduction and the heat stored in the reservoir. While most parameters can be estimated, the reservoir volume remains unknown. However, it is possible to estimate the required reservoir size based on different scenarios of formation temperature changes. In Fig. 13, the reservoir area needed to account for the historical thermal output of the field is calculated, with the parameters summarized in Table 1.

Without any heat extraction ($\Delta T_R = 0$), unrealistically large reservoir areas would be required to satisfy the energy balance during production.

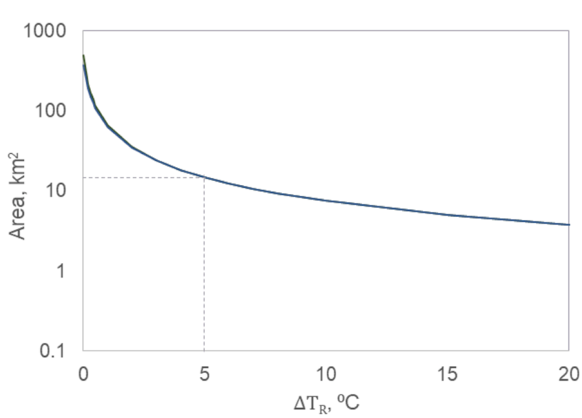


**Fig. 13.** Calculated reservoir area to resolve heat balance with conductive heat flux and stored heat as heat sources.

This suggests that basal conduction alone cannot sustain the thermal output of the field. However, incorporating some degree of formation cooling allows the energy balance to be resolved with more realistic area estimates. For instance, cooling the topmost 0.5 km of an area of 17 km$^2$ by 5 °C is sufficient to sustain the productive life of the field. Although the reservoir exhibits ~2 km of convective temperatures, only the topmost 0.5 km is considered, as this represents the zone where the majority of the temperature change occurs. The calculated area (or volume of rocks) includes not only the reservoir rocks, but also the rocks outside of the reservoir where recharge streams could potentially absorb heat.

Fig. 13 also implies that the heat balance of the field is largely controlled by the extraction of stored heat. The steep decline in the calculated area suggests that the contribution of conductive heat flux is negligible compared to the stored heat, suggesting that the stored heat is the primary heat source of the field. The stored heat term in Eq. (4) may also be applied to discretized vertical layers, along with observed and modeled temperature decline shown in Fig. 11. The larger $\Delta T_R$ in the shallower sections suggests that most of the heat is extracted from these layers. Consequently, the productive layers at depth are largely unaffected, which may explain the near-constant discharge temperatures observed.

While distributed heat extraction from near-surface rocks at Laugarnes masks the thermal decline in deeper production zones, the inflow of colder recharge with higher flow velocities or more focused recharge structures would prevent the recharging fluid to thermally equilibrate with a large volume of rock, leading to more rapid thermal decline. Observations from various high-temperature (Bixley et al., 2009; Glover and Mroczek, 2009; Sunio et al., 2010; Clemente and Villadolid-Abrigo, 1993; Gambill and Beraquit, 1993; Menzies et al., 2010;) and low-temperature (Tómasson, 1993; Axelsson 2010) geothermal fields show that the extent of cold inflows on production depends on reservoir conditions and the extent of inflow. These differences highlight the importance of understanding recharge dynamics and their dependence on geologic and reservoir controls in both low- and high-temperature geothermal systems.

### 5.2. Revised conceptual model of the laugarnes system

The observed “top-down” temperature decrease, along with its associated energy equivalent, suggests that the influx of cold, shallow recharge into the reservoir is the primary driver of heat transport during production. This highlights the significant role of the recharge in shaping the thermal behavior of the system. In Fig. 14, we present an updated conceptual model of the field incorporating the shallow recharge during production.

In Fig. 14a, the thermal structure of the natural state is primarily controlled by the deep flow of water from the southeast and rises beneath Laugarnes. The recharge direction may then explain the low salinity of water from the Laugarnes wells, which contain only around 35 ppm dissolved Cl (Arnórsson, 1995), despite the area being almost surrounded by the sea from the northwest to the east. This flow, largely driven by topography, encounters higher permeability beneath Laugarnes, which allows water to rise, and to some extent flow laterally toward the east and northeast. The eastward outflow may explain the temperature reversal observed in the deep well to the east of the field (Fig. 9f). If this outflow extends further east, it may also account for temperature reversals as far as Elliðaár (Tómasson, 1993).

The topography-driven flow from the southeast contrasts with the previous conceptual model of Björnsson et al. (1999, 2000, Fig. 5), which proposed deep recharge from the northeast. Their interpretation suggests that permeability is controlled by NE-SW fractures and may explain the newly identified blind geothermal systems at Geldinganes (northeast of Laugarnes) and Kjalarnes (further north-northeast). This fracture system must be effectively sealed at the top because it runs beneath the sea; otherwise, seawater intrusion would have significantly

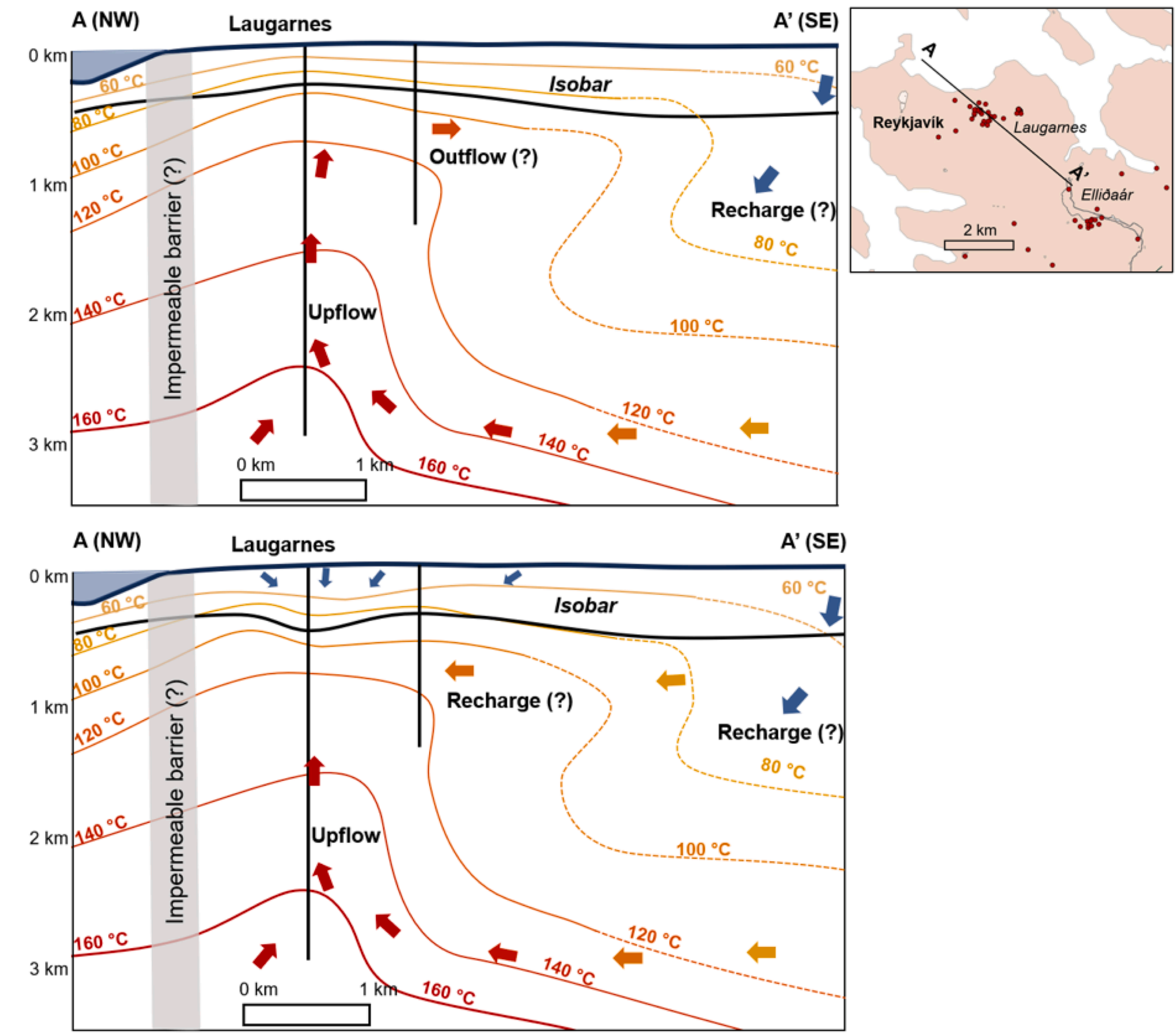


**Fig. 14.** A revised conceptual model of Laugarnes in (a) the initial state and (b) the produced state.

increased salinity at Laugarnes. Additionally, this fracture orientation contradicts water level drawdown mapped by Thorsteinsson and Elíasson (1970), where pressure contours showed elongations in a NW-SE direction – perpendicular to the fractures proposed in the previous model. In contrast, this water level pattern aligns with the recharge suggested in the conceptual model presented in this study.

These contrasting interpretations highlight the need for further investigation into the origins of hot water recharge in the natural state. A possible hydraulic connection between Laugarnes and Geldinganes or Kjalarnes (NE-SW) could be tested through tracer studies, as could a connection between Laugarnes and Elliðaár (NW-SE). Despite these differences, the shallow recharge during production may still hold true, and we explore this further in the following text.

As water is extracted during production, the resulting drawdown creates a driving force for recharge waters to flow into the reservoir. In Fig. 14b, this is represented as a depression in the isobar. In the absence of an overlying low-permeability layer, such as a clay cap, surface water can freely infiltrate the reservoir. The drawdown may also reverse the original outflow direction, causing water to be drawn from the reservoir's periphery. The heat extraction associated with this recharge cools the formation, as reflected in the isotherm depressions at locations where recharge occurs. Similar depressions in the isobar and isotherms are implemented in Elliðaár, which may explain the temperature decline that are recorded from the wells as shown by Bravo (2024).

The thermal structure and recharge flow shown in Fig. 14 are derived from numerical model results, calibrated by adjusting the anisotropic permeabilities of various lithologic units. This underscores the role of the calibrated anisotropic permeabilities, summarized in Table 3, in

**Table 3**
Rock and water properties used in energy balance calculations.

| Parameter | Value | Source |
|---|---|---|
| $C_R$, Rock heat capacity | 1050 J kg$^{-1}$ °C$^{-1}$ | Sigurdson and Stefansson (1994) |
| $\rho_R$, Rock density | 2890 kg m$^{-3}$ | |
| Φ, Active porosity | 7 % | |
| $C_w$, Water heat capacity | 4000 J kg$^{-1}$ °C$^{-1}$ | Average steam table values from 5–120 °C |
| $\rho_w$, Water density | 940 kg m$^{-3}$ | |
| h, reservoir thickness | 500 m | |

governing the transport of heat and mass during both the initial state and production phases. Generally, changes in permeabilities had opposing effects on the two calibration parameters: natural-state temperatures and production history pressures. Lowering permeabilities reduced water convection, which, to some extent, trapped more heat within the blocks and resulted in higher natural-state temperatures. However, during production calibration, lower permeability restricted mass exchange between blocks, leading to a greater decline in reservoir pressures. Consequently, the permeability values needed to balance these effects: they had to be low enough to replicate natural-state temperatures accurately but high enough to allow sufficient mass transfer between blocks to sustain hot water production. The reservoir permeability values in Table 3, on the order of $10^{-14}$ $m^2$, agree well with those from previous analytical and lumped-parameter models (Bodvarsson and Zais, 1981; Björnsson et al., 1990; Changhong, 2012). This suggests that the numerical model effectively replicates the performance and predictions of the analytical models developed in the past.

The vertical permeability ($k_z$) of the global and reservoir rocks was set two to four times lower than their lateral permeabilities ($k_x$ and $k_y$), which drives water to flow more laterally and allows it to heat progressively along its path. Although the water gains buoyancy as it heats, the reduced vertical permeability restricts upward flow until it reaches zones of enhanced vertical permeability in the reservoir, as shown in Fig. 14a. This permeability pattern may reflect the depositional history of the rocks, where successive subaerial and subglacial lava flows create layered structures (Thorsteinsson and Elíasson, 1970; Friðleifsson, 1990), with interlayer contacts acting as preferential pathways. In contrast, the increased permeability in Laugarnes may result from recent fracturing of the deposited rocks.

The lower vertical permeability within the reservoir acts as a mechanism to retain pressure, allowing an overpressure of 7 barg to develop in the natural state, even without a low-permeability layer such as a clay cap. This overpressure, illustrated by the slight increase in the isobar in Fig. 14a, is driven by buoyant forces resulting from the density difference between the reservoir fluid and the surrounding cooler aquifers. The absence of a clay cap aligns with the lithostratigraphy described in Thorsteinsson and Elíasson (1970) and Friðleifsson (1990). Despite the lack of a confining layer, the numerical model successfully replicates the initial-state overpressure due to the sufficiently low vertical permeability. Simultaneously, the permeability remains high enough to sustain convective upflow, as reflected in the modeled isothermal natural-state temperatures observed in wells (Fig. 9). This suggests that the assumed permeability effectively balances its opposing effects on pressure and temperature during natural-state calibration.

The absence of a clay cap then implies that the reservoir is unconfined. This modeling approach assumes that the reservoir is connected to a constant-pressure outer boundary, represented by the atmosphere in this case. In the numerical model, this was implemented by connecting the topmost blocks to the atmosphere set at constant pressure and temperature. As a result, shallow recharge can infiltrate the reservoir during production, consistent with the open-boundary interpretations of earlier analytical models (Thorsteinsson and Elíasson, 1970; Bodvarsson and Zais, 1981; Axelsson, 1989; Fendek, 1992; Sarak et al., 2005; Changhong, 2012). In this context, an open boundary assumes that the reservoir is connected to a recharge source with constant pressure (Sarak et al., 2005).

This connection to a shallow open boundary condition then implies a balance in vertical permeability: it must be high enough to allow water infiltration into the system, yet low enough to slow the associated thermal cooling. The historical pressure match in the numerical model (Fig. 10) illustrates that the recharge is sufficient. Similarly, the modeled temperature decline (Fig. 11) shows that the resulting thermal cooling within the rocks, caused by the cold recharge, aligns with the observed cooling measured in the wells. Notably, this temperature decline was not used in the calibration but served as a check on the model's predictive capability. These results demonstrate that the calibrated permeability distribution achieves the necessary balance during production-history calibration: providing sufficient recharge while mitigating the downward movement of a thermal front.

The historical reservoir pressure match in the numerical model demonstrates that it satisfies the field's mass balance. However, attributing pressure support solely to shallow recharge would be incorrect. Although no basal mass input was included in the numerical model, upflow still occurs due to natural convection of water. The potential for upflow is further increased during production as pressure decreases. However, because the upflow is driven by natural convection (Fig. 14a), the flow is ultimately limited by the permeability distribution of both the reservoir and surrounding rocks. This suggests that the primary pressure support for the system during production is the recharge from the surface, implying that the heat produced by the field primarily results from shallow formation cooling.

The role of formation cooling as the primary heat source has significant implications for the sustainability and longevity of the field as a hot water source for the city. Cold recharge extracting heat from the shallow formations suggests a downward-moving thermal front over time, which could eventually affect the deeper, more productive sections of the reservoir. However, forecasts from the numerical model (Fig. 12b) indicate that as long as current production levels are maintained, the average discharge temperature will decrease only by 5 °C over the next century. This implies that while there is decline, the impacts may remain within an acceptable range. Increasing production, on the other hand, may enhance the movement of the thermal front, potentially leading to worse temperature decline. Despite these findings, we acknowledge the limitations of the existing model and emphasize the need for improvements to better predict future reservoir performance.

### 5.3. Heat source and origins of low-temperature systems

Our modeling suggests that elevated regional heat flux alone can reproduce the natural-state upflow and temperature profiles in Laugarnes. This challenges the prevailing assumption that convective downward migration (CDM) is required to sustain the heat output of large low-temperature fields – such as Laugarnes, which has maintained an annual average heat output of 80 $MW_{th}$ over the past 50 years. We present that instead of a fracture progressively opening downward, a similar mechanism could support high heat output of geothermal fields where recharge water progressively cools down shallower sections.

In some ways, our model revisits the concept first proposed by Einarsson (1966), which attributes low-temperature systems solely to the high conductive heat flux in the region. However, instead of assuming steady-state heat flow, which would require large expanse of conductive area to satisfy the energy balance of Einarsson's model, we propose that the top-down heat extraction from the shallow formation by cold recharge is sufficient to sustain the high thermal output during production.

This mechanism suggests that in the natural-state, heat is extracted from a large volume of rock at depth and discharged through natural water convection into upflow zones located in areas of higher permeability. Such a system may form if the surrounding rocks have relatively lower vertical permeability, which prevents heated water from moving upward. Instead, the heat is localized in areas with intensified permeability, where structures such as fractures play a crucial role in concentrating permeability (Jolie et al., 2021), and consequently, the heat extracted. In the case of Laugarnes and other low-temperature systems in the Reykjavík area, the higher permeability may result from the interplay of fracture zones intersecting the caldera rim (Gunnlaugsson et al., 2000; Arnórsson et al., 1992; Tómasson, 1993), as shown in Fig. 2.

This heat flow mechanism may explain the temperature profiles of wells drilled in the low-temperature fields, where deeper sections are colder than the undisturbed rocks, while the shallower sections are hotter (Fig. 1). This has previously been interpreted as "thermal mining" from the base of the systems, with heat then being transported to the shallower sections (Tómasson and Arason, 2000). Alternatively, such temperature profile could also result from heat being extracted from a larger area and is channeled into a smaller, high-permeability zone. In these high-permeability areas (i.e., geothermal fields), convection is strong enough such that the heat is redistributed to the shallower sections. The natural-state numerical modeling of Laugarnes (Fig. 8) demonstrates this process.

This heat flow mechanism also implies that some areas surrounding the reservoir must have a temperature regime lower than the background geothermal gradient of 90–120 °C/km (Fig. 1, Well 3). In these areas, the surrounding rocks lose heat to water that is being transported into the upflow zones. As a result, the water remains cold, dense, and tends to downflow. Cold-water systems of this nature near the Reykjavík systems have already been identified through temperature surveys of wells in Garðabær, just a few kilometers south of Reykjavík, and in Kaldársel, further south (Björnsson et al., 1999). Wells drilled in these areas show cold water downflowing to depths of at least 750–1000 m, despite their proximity to the volcanically active region further southeast (Tómasson, 1993).

To some extent, the heat flow model presented in this study shares similarities with the CDM model, with the key difference being that the primary areas of heat extraction are located at the system's margins rather than its base. The CDM model depicts these convection cycles as closed and narrowly localized along faults or fractures. Reconciling the downward migration of a fracture in a high-temperature area with the presence of hot upflow is challenging, as buoyancy would cause the water to ascend. Only cold, dense surface water tends to descend, and this effect becomes more pronounced following reservoir depressurization. In sustaining the thermal output of Laugarnes during production, our model does not rely on the downward-propagating heat extraction at the base emphasized in the CDM model, but rather on heat extraction in the shallower sections.

Still, this heat flow model struggles to explain low-temperature fields with very high natural-state thermal output, such as Reykholtsdalur (220 $MW_{th}$), unless a thermal decline is already occurring over time, even in the absence of external mass extraction (production). So far, we have assumed that pre-production conditions in Laugarnes (3 $MW_{th}$) are at stead-state. Assuming the same for Reykholtsdalur would require an unrealistically large area of about 2000 $km^2$ (Bodvarsson, 1982a) to sustain its heat output. However, steady-state conditions may not be necessary, especially for very large low-temperature geothermal systems. These systems could already be undergoing transient cooling before production, akin to the process underlying the CDM model, but with extraction occurring in the top or margins rather than being confined to the base. Our calculations and numerical model show that once heat extraction from the rocks is incorporated, it becomes the dominant heat source, as observed in Laugarnes during production.

The heat flow model presented does not necessarily contradict the CDM model in explaining the natural state of low temperature geothermal systems. The CDM model may still play a significant role, particularly in fields with very high natural state thermal output. In the case of Reykholtsdalur, Bodvarsson (1982a) accounted for the 220 MWth heat output by assuming the presence of several dikes with a combined fracture length of 40 km. A possible interpretation integrates both heat transport mechanisms: CDM may govern the formation of low temperature systems, while top-down cooling becomes dominant once production induced drawdown begins. To further evaluate the CDM model, static temperature surveys could be carried out in wells that extend to the base of the system to monitor the progression of the isothermal zone. Although such data are currently unavailable, primarily because most deep wells are equipped with downhole pumps, this approach could be reconsidered in the future. Interference tests between Laugarnes and fields located several kilometers away along the proposed CDM pathway are currently ongoing and may reveal whether connectivity exists. To investigate the proposed distributed permeability recharge, tracer tests could be conducted using the available idle wells, many of which are shallow and located near the production area. These tests may help clarify the role of distributed permeability in facilitating recharge.

Heat extraction may not be confined solely to geothermal fields but could also occur in recharge zones, potentially extending beyond the system itself. If these recharge zones intersect sufficiently hot rocks, such as undisturbed geothermal formations, there is significant potential for heat exchange to occur. As a result, low-temperature geothermal systems, including those with very high thermal output, may form in areas where water has access to unusually hot rocks along distributed recharge pathways.

## 6. Conclusions

This study examined long-term production and field data from Laugarnes, leading to a reevaluation of the field's conceptual model based on the findings. To quantitatively assess the revised model, both a simple overall energy balance and a numerical model were developed. The key findings include:

- A "top-down" cooling pattern is observed from the wells, suggesting the presence of a shallow cold recharge influx that extracts heat as it percolates into the deeper, productive sections of the reservoir.
- Energy balance calculations suggests that the formation cooling associated with the influx of shallow waters is sufficient to account for the historical heat output of the field.
- The conceptual model of the field was updated to include the shallow recharge mechanism. In the numerical model, the natural-state temperatures, pressure history, and the shallow formation temperature decline were successfully replicated. This further demonstrates how the proposed mechanism is sufficient to support the mass and heat transport in the field.

The new conceptual model presents an alternative framework for understanding heat flow in Laugarnes, with implications for its longevity and sustainability. While previous conceptual and quantitative models suggest the field could be operated indefinitely without significant thermal decline, the new model introduces the possibility of a migrating thermal front originating at the surface. Our modeling indicates that the reservoir structure of Laugarnes allows this front to move slowly, meaning that even after 100 years of production, the discharge temperatures of the wells remain largely unaffected. However, this front could eventually impact the deeper, productive sections of the reservoir, underscoring the need to refine the model for more accurate predictions of the field's future performance. This also highlights the importance of temperature measurements from the wells to further confirm if thermal migration is present, Nonetheless, the model suggests that, in the foreseeable future, thermal decline is unlikely to significantly affect discharge temperatures in the field.

The conceptual model also provides valuable insights on the origins and mechanisms sustaining low-temperature geothermal fields, highlighting how formation cooling could be an important heat source for these fields. While this phenomenon is observed in Laugarnes, similar processes may be happening in other low-temperature fields. For example, systems with shallower feed zones may not exhibit the stable discharge temperatures observed in Laugarnes. Therefore, incorporating formation cooling into forecasts is essential for accurately predicting the longevity of these fields. Understanding this mechanism is critical in assessing the sustainability of the low-temperature fields, especially because these fields are vital to the district heating across the entire country.

## CRediT authorship contribution statement

**Adolph Bravo:** Writing – review & editing, Writing – original draft, Visualization, Resources, Project administration, Methodology, Investigation, Formal analysis, Data curation, Conceptualization. **Samuel Scott:** Writing – review & editing, Writing – original draft, Visualization, Supervision, Resources, Methodology, Investigation, Funding acquisition, Formal analysis, Data curation, Conceptualization. **Halldór Pálsson:** Writing – review & editing, Supervision, Project administration, Methodology, Investigation, Formal analysis, Conceptualization. **Gunnar Gunnarsson:** Writing – review & editing, Validation, Supervision, Resources, Methodology, Investigation, Formal analysis, Data curation, Conceptualization.

## Declaration of competing interest

The authors declare that they have no known competing financial interests or personal relationships that could have appeared to influence the work reported in this paper.

## Acknowledgments

This project was funded by the Energy Research and Innovations Fund of Orkuveitan (VOR) through grant agreement SAM-2023–1362. The authors also thank Orkuveitan for providing access to field data.

## Data availability

Data will be made available on request.

## References

Árnason, B., 1977. Hydrothermal systems in Iceland traced by deuterium. Geothermics 5 (1–4), 125–151. https://doi.org/10.1016/0375-6505(77)90015-3.

Arnórsson, S., 1995. Geothermal Systems in Iceland: structure and conceptual models—II. low-temperature areas. Geothermics 24 (5–6), 603–629. https://doi.org/10.1016/0375-6505(95)00026-7.

Arnórsson, S., Björnsson, S., Jóhannesson, H., Gunnlaugsson, E., 1992. Vinnslueiginleikar lághitasvæða Hitaveitu Reykjavíkur (The production characteristics of the low-temperature reservoirs of the Reykjavík Municipal District Heating Service). VFÍ Yearbook 344–366. https://timarit.is/issue/356950.

Axelsson, G., 1985. Hydrology and thermomechanics of liquid-dominated hydrothermal systems in Iceland [Doctoral dissertation. Oregon State University. https://ir.library.oregonstate.edu/concern/graduate_thesis_or_dissertations/ms35tc96f.

Axelsson, G., 1989. Simulation of pressure response data from geothermal reservoirs by lumped-parameter models. In: Proceedings of the 14th Workshop on Geothermal Reservoir Engineering. Stanford University, Stanford, California, pp. 257–263.

Axelsson, G., 2010. Sustainable geothermal utilization – case histories; definitions; research issues and modelling. Geothermics 39 (4), 283–291. https://doi.org/10.1016/j.geothermics.2010.08.001.

Axelsson, G., Gunnlaugsson, E., Jónasson, T., Ólafsson, M., 2010. Low-temperature geothermal utilization in Iceland – decades of experience. Geothermics 39 (4), 329–338. https://doi.org/10.1016/j.geothermics.2010.09.002.

Beaude, L., Brenner, K., Lopez, S., Masson, R., Smai, F., 2019. Non-isothermal compositional liquid gas darcy flow: formulation, soil-atmosphere boundary condition and application to high-energy geothermal simulations. Computational Geosciences 23 (3), 443–470. https://doi.org/10.1007/s10596-018-9794-9.

Bixley, P.F., Clotworthy, A.W., Mannington, W.I., 2009. Evolution of the wairakei geothermal reservoir during 50 years of production. Geothermics 38 (1), 145–154. https://doi.org/10.1016/j.geothermics.2008.12.007.

Björnsson, A., Axelsson, G., Olafur, F., 1990. Uppruni hvera og lauga á Íslandi (The nature of hot spring systems in Iceland). Náttúrufræðingurinn 60, 15–38.

Björnsson, G., Thordarson, S., & Steingrímsson, B. (1999). *Hiti í berggrunni og hugmyndalíkan af jarðhitakerfum á höfuðborgarsvæðinu (Report No. OS-99112, Heat in bedrock and a conceptual model of geothermal systems in the capital area)*. Reykjavík, Iceland: Orkustofnun. http://hdl.handle.net/10802/19785.

Björnsson, G., Thordarson, S., Steingrímsson, B., 2000. Temperature distribution and conceptual reservoir model for geothermal fields in and around the City of Reykjavík, Iceland. In: Proceedings of the 25th Workshop Geothermal Reservoir Engineering. Stanford, California.

Bodvarsson, G., 1982a. Glaciation and geothermal processes in Iceland. Jökull 32, 21–28.

Bodvarsson, G., 1982b. Terrestrial energy currents and transfer in Iceland. Geodynamics Series 271–282. https://doi.org/10.1029/gd008p0271.

Bodvarsson, G., 1983. Temperature/flow statistics and thermomechanics of low-temperature geothermal systems in Iceland. Journal of Volcanology and Geothermal Research 19 (3–4), 255–280. https://doi.org/10.1016/0377-0273(83)90114-2.

Bodvarsson, G., Zais, E., 1981. A field example of free surface testing. Journal of the Icelandic Society of Engineers 66, 92–95. https://timarit.is/issue/348644.

Bravo Jr., A., 2024. Heat Flow Modeling of the Laugarnes and Elliðaár Geothermal Fields [Master's thesis. University of Iceland. Reykjavík. https://hdl.handle.net/1946/46259.

Changhong, F., 2012. Reservoir Parameter Estimates and Water Level Predictions for the Laugarnes Low-temperature System, SW-Iceland, by Simple Analytical and Lumped-parameter Models (Report No. UNU-GTP-2012-09). UNU-GTP, Reykjavík, Iceland. http://www.os.is/gogn/unu-gtp-report/UNU-GTP-2012-09.pdf.

Clearwater, J., Franz, P., 2019. Introducing the Volsung Geothermal Simulator: features and applications. In: Proceedings of the 41st New Zealand Geothermal Workshop. Auckland, New Zealand.

Clemente, W.C., Villadolid-Abrigo, F.L., 1993. The Bulalo Geothermal Field, Philippines: reservoir characteristics and response to production. Geothermics 22 (5–6), 381–394. https://doi.org/10.1016/0375-6505(93)90026-j.

Croucher, A., 2011. PyTOUGH: a Python scripting library for automating TOUGH2 simulatioins. In: Proceedings of the 33rd New Zealand Geothermal Workshop. Auckland, New Zealand.

Einarsson, T., 1966. Um orsakir jarðhitans (On the nature of geothermal fields). Tímarit VFÍ 51, 23–32.

Fendek, M., 1992. Distributed Parameter Models for the Laugarnes Geothermal Field, SW-Iceland and the Central Depression of Danube Basin, S-Slovakia (Report No. UNU-GTP-1992-05). UNU-GTP, Reykjavík, Iceland. https://gogn.orkustofnun.is/unu-gtp-report/UNU-GTP-1992-05.pdf.

Flóvenz, Ó.G., Saemundsson, K., 1993. Heat flow and geothermal processes in Iceland. Tectonophysics 225 (1–2), 123–138. https://doi.org/10.1016/0040-1951(93)90253g.

Franz, P., Clearwater, J., 2021. Volsung: a comprehensive software package for geothermal reservoir simulations. In: Proceedings World Geothermal Congress 2020 +1. Reykjavik, Iceland.

Friðleifsson, O.G., 1982. Reykjavík Hola RG-38: Borun, jarðlög, og ummyndun (Report No. OS-82034, Reykjavík well RG-38: Drilling, formation, and alteration). Orkustofnun, Reykjavík, Iceland. https://gogn.orkustofnun.is/Skyrslur/OS-1982/OS-82034.pdf.

Friðleifsson, O.G., 1990. Jarðfræði Laugarnessvæðisins í Reykjavík (Report No. OS-90035, Geology of the Laugarnes area in Reykjavik). Orkustofnun, Reykjavík, Iceland. https://gogn.orkustofnun.is/Skyrslur/OS-1990/OS-90035.pdf.

Gambill, D.T., Beraquit, D.B., 1993. Development history of the Tiwi Geothermal Field, Philippines. Geothermics 22 (5–6), 403–416. https://doi.org/10.1016/0375-6505(93)90028-l.

Glover, R.B., Mroczek, E.K., 2009. Chemical changes in natural features and well discharges in response to production at Wairakei, New Zealand. Geothermics 38 (1), 117–133. https://doi.org/10.1016/j.geothermics.2008.12.008.

Grant, M.A., Bixley, P.F., 2011. Simple quantitative models. Geothermal Reservoir Engineering 29–60. https://doi.org/10.1016/b978-0-12-383880-3.10003-4.

Gunnlaugsson, E., Gislason, G., Ivarsson, G., Kjaran, S.P., 2000. Low temperature geothermal fields utilized for district heating in Reykjavík, Iceland. In: Proceedings of the World Geothermal Congress 2000. Kyushu-Tohoku, Japan.

Halldórsdóttir, S., Berre, I., Keilegavlen, E., Axelsson, G., 2023. Crustal conditions favoring convective downward migration of fractures in deep hydrothermal systems. Geophys Res Lett 50 (22). https://doi.org/10.1029/2023gl105380.

Jolie, E., Scott, S., Faulds, J., Chambefort, I., Axelsson, G., Gutiérrez-Negrín, L.C., Regenspurg, S., Ziegler, M., Ayling, B., Richter, A., Zemedkun, M.T., 2021. Geological controls on geothermal resources for Power Generation. Nat Rev Earth Environ 2 (5), 324–339. https://doi.org/10.1038/s43017-021-00154-y.

Kristmannsdóttir, H., 1975. Hydrothermal alteration of basaltic rocks in Icelandic geothermal areas. In: Proceedings of the second United Nations symposium on the development and use of geothermal resources. San Francisco, California.

Lund, J.W., Toth, A.N., 2021. Direct utilization of Geothermal energy 2020 Worldwide Review. Geothermics 90, 101915. https://doi.org/10.1016/j.geothermics.2020.101915.

Melsted, O., 2021. Eliminating fossil fuels: iceland's transition from coal and oil to geothermal district heating, 1930–1980. Hist Technol 37 (4), 527–547. https://doi.org/10.1080/07341512.2022.2033386.

Menzies, A.J., Villaseñor, L.B., Sunio, E.G., 2010. Tiwi Geothermal Field, Philippines: 30 years of commercial operation. In: Proceedings World Geothermal Congress 2010. Bali, Indonesia.

O'Sullivan, M.J., O'Sullivan, J.P., 2016. Reservoir modeling and simulation for Geothermal Resource Characterization and Evaluation. Geothermal Power Generation 165–199. https://doi.org/10.1016/b978-0-08-100337-4.00007-3.

Patterson, J.W., Driesner, T., 2021. Elastic and thermoelastic effects on thermal water convection in fracture zones. Journal of Geophysical Research: Solid Earth 126 (2). https://doi.org/10.1029/2020jb020940.

Quinao, J.J., Zarrouk, S.J., 2014. A review of the volumetric stored-heat resource assessment: one method, different results. In: Proceedings 36th New Zealand Geothermal Workshop. Auckland, New Zealand.

Ragnarsson, Á., Steingrímsson, B., Thorhallsson, S., 2023. Geothermal development in Iceland 2020-2022. In: Proceedings World Geothermal Congress 2023. Beijing, China.

Ratouis, T.M.P., O'Sullivan, M.J., O'Sullivan, J.P., 2016. A numerical model of Rotorua Geothermal Field. Geothermics 60, 105–125. https://doi.org/10.1016/j.geothermics.2015.12.004.

Sarak, H., Onur, M., Satman, A., 2005. Lumped-parameter models for low-temperature geothermal fields and their application. Geothermics 34 (6), 728–755. https://doi.org/10.1016/j.geothermics.2005.09.001.

Sunio, E.G., Menzies, A.J., Alvarez, R.R., Lim, W.Q., Stark, M.A., 2010. Downflows in wells at the Mak-Ban Geothermal Field, Philippines. In: Proceedings World Geothermal Congress 2015. Melbourne, Australia.

Thorbergsson, E.M., Fridriksson, T., Sverrisdottir, S.M., Adalsteinsdottir, H., Tryggvadottir, L., Bjornsson, G.B., Palsdottir, A., Davidsson, S.H., Gunnarsson, H., 2023. The 100-year plan – A long term vision for sustainable resource management in district heating. In: Proceedings World Geothermal Congress 2023 Beijing, China. *April 17 –21, 2023*.
Thorsteinsson, T., Elíasson, J., 1970. Geohydrology of the laugarnes hydrothermal system in Reykjavík, Iceland. Geothermics 2, 1191–1204. https://doi.org/10.1016/0375-6505(70)90432-3.
Tómasson, J., 1993. The nature of the Ellidaár geothermal area in SW-iceland. Geothermics 22 (4), 329–348. https://doi.org/10.1016/0375-6505(93)90006-9.
Tómasson, J., Arason, P., 2000. Evidence for thermal mining in low temperature geothermal areas in Iceland. Geothermics 29 (6), 723–735. https://doi.org/10.1016/s0375-6505(00)00030-4.
Tómasson, J., Friðleifsson, I.B., Stefánsson, V., 1975. A hydrological model for the flow of thermal water in SW-Iceland with a special reference to the Reykir and Reykjavík thermal areas. In: Proceedings of the second United Nations symposium on the development and use of geothermal resources. http://hdl.handle.net/10802/21922.
Yaowanoiyothin, W., 1984. Hydrothermal Alteration in Borehole RV-40 (Report No. UNU-GTP-1984-12). UNU-GTP, Reykjavík, Iceland. https://gogn.orkustofnun.is/unu-gtp-report/UNU-GTP-1984-12.pdf.